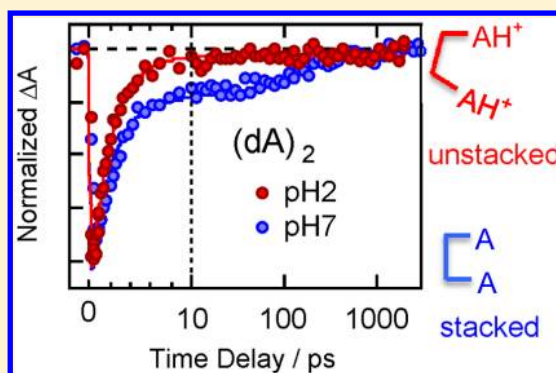


Base-Stacking Disorder and Excited-State Dynamics in Single-Stranded Adenine Homo-oligonucleotides

Charlene Su,[†] Chris T. Middleton,^{†,§} and Bern Kohler^{*,‡}[†]Department of Chemistry, The Ohio State University, 100 West 18th Avenue, Columbus, Ohio 43210, United States[‡]Department of Chemistry and Biochemistry, Montana State University, Bozeman, Montana 59717-3400, United States

S Supporting Information

ABSTRACT: Single-stranded adenine homo-oligonucleotides were investigated in aqueous solution by femtosecond transient absorption spectroscopy in order to study the effect of strand length on the nature and dynamics of excited states formed by UV absorption. Global fitting analysis of bleach recovery signals recorded at a probe wavelength of 250 nm and pH 7 reveals that the same lifetimes of 2.72 and 183 ps reproduce the pronounced biexponential decays observed in all $(dA)_n$ oligomers, containing between 2 and 18 residues. Although the lifetimes are invariant, the amplitudes of the short- and long-lived components depend sensitively on the number of residues. For example, the 183 ps component increases with strand length and is greater for DNA vs RNA single strands with the same number of adenines. Inhomogeneous kinetics arising from two classes of adenine bases in each oligomer best explains the observations. A subset of adenine residues produce short-lived excited states upon excitation, while absorption by the remaining adenines yields long-lived excited states that are responsible for the long-lived signal. By assuming that each short-lived excited state in the oligomer makes the same contribution to the transient absorption signal as an excited state of the adenine mononucleotide, the fraction of each type of base in the oligomer can be estimated along with the quantum yield of long-lived excited states. The fraction of oligonucleotides that yield long-lived excited states increases with oligomer length in precisely the same manner as the fraction of bases that are found in base stacks. Corroborating evidence that base stacking leads to distinct decay channels comes from experiments conducted at low pH on $(dA)_2$. Coulombic repulsion between the two protonated bases at pH 2 results in open, unstacked conformations causing the long-lived component seen in $(dA)_2$ at neutral pH to vanish completely. The fast component seen in oligomers with two or more bases is assigned to vibrational cooling following ultrafast internal conversion to the electronic ground state. This monomer-like decay channel is operative for the subset of adenine residues that are either poorly or not at all stacked with neighboring bases. This study shows that static base stacking disorder fully accounts for the length-dependent transient absorption signals. Although absorption likely creates delocalized excitons of unknown spatial extent, the results from this study suggest that long-lived excitations in single-stranded A tracts are already fully localized on no more than two bases no later than 1 ps after UV excitation.



1. INTRODUCTION

Femtosecond spectroscopy has dramatically advanced understanding of photophysical and photochemical decay pathways of excited electronic states in nucleic acids.^{1–3} Knowledge of these pathways is crucial for understanding the initial events behind UV damage to DNA. Although there is growing consensus about photophysical decay mechanisms in single bases, the nature and dynamics of excited states in assemblies of two or more bases—the so-called base multimers—is the subject of considerable debate.⁴ Transient absorption experiments performed on base multimers ranging from dinucleosides⁵ to single-stranded homopolymers composed of several hundred nucleotides⁶ reveal longer lifetime components of several picoseconds to as much as several hundred picoseconds. Although they decay in a fraction of a nanosecond, these states are termed long-lived excited states to emphasize the contrast with the subpicosecond excited state lifetimes generally seen for

single bases. Long-lived excited states are also seen in transient absorption signals from double-stranded DNA oligomers,^{7–11} and a nanosecond lifetime was recently observed for a microhydrated adenine cluster $A_2(H_2O)_3$.¹² Complex, multi-exponential decays have also been observed in time-resolved emission experiments.^{13–15}

Different explanations for the long-lived singlet excited states observed in DNA have been discussed in the literature.⁴ Kwok et al.¹⁶ concluded that long-lived excited states in $(dA)_{20}$ are delocalized excimer states populated from initial excitations that are strongly localized. On the other hand, Buchvarov et al.¹⁷ assigned their transient absorption signals from variable-length $(dA)_n$ oligomers to delocalized Frenkel excitons, which they

Received: June 1, 2012

Revised: July 31, 2012

Published: August 1, 2012



argue span a number of neighboring bases. Recently, Conti et al.¹⁸ argued that long-lived excitations in DNA could be localized on just a single nucleobase. They presented calculations which suggest that a nucleobase within a base stack experiences sufficient steric hindrance to impede the out-of-plane motions responsible for ultrafast nonradiative decay.¹⁸ On the other hand, we have concluded from our experiments that long-lived excited states are localized on two bases, consistent with charge transfer or excimer states.⁴

Given the persistent uncertainty about the nature and spatial extent of excited states in DNA oligomers, we present and analyze new femtosecond transient absorption signals from variable-length single-stranded adenine homo-oligonucleotides and critically examine what the signals reveal about excited states formed in these systems by UV light. We emphasize in our analysis the implications of a finding that appears to have been overlooked by many workers in DNA electronic structure theory: Single-stranded DNAs are structurally heterogeneous at room temperature and consist of helical domains of stacked bases interrupted by bases that are unstacked. Here, we present experiments that show how static structure, specifically length-dependent base stacking, fully explains the observed signal variation with oligomer length, and we argue that these signals do not provide evidence of delocalized excitons.

2. EXPERIMENTAL METHODS

Femtosecond transient absorption experiments were carried out using a 1 kHz Ti:sapphire laser system manufactured by Coherent Inc. The pulses from a regenerative amplifier were split into pump and probe pulses. The pump wavelength at 266 nm was obtained through third harmonic generation of the fundamental wavelength, and the probe wavelength at 250 nm was generated using an optical parametric amplifier. The pump and probe beams were spatially overlapped in a home-built spinning cell with CaF₂ windows and a path length of 1.2 mm. The polarization of the probe beam was set at the magic angle (54.7°) relative to the polarization of the pump beam for measuring reorientation-free signals. Probe pulses were spectrally filtered after the sample using a compact double monochromator and detected by a photomultiplier tube. A lock-in amplifier referenced to the 333 Hz signal from an optical chopper placed in the pump beam measured the absorbance change in the probe beam. The 3 μ J pump pulses were focused to a diameter of 1200 μ m in the sample solution. This spot size was large enough to avoid multiphoton excitation and photodegradation. The probe pulses had 2 to 3 orders of magnitude less energy and were focused to a beam diameter of 300 μ m in the sample.

Samples. Multimers with DNA sugars are indicated with a “d” for 2′-deoxyribose, as in (dA)₂. RNA oligomers in which the ribose group has a hydroxyl group at the 2′ carbon are denoted with an “r”, as in (rA)₂, in order to better distinguish them from the DNA forms.¹⁹ AMP (adenosine 5′-monophosphate, 99+% purity), dAMP (2′-deoxyadenosine 5′-monophosphate, sigma grade, 98+% purity), poly(rA) (polyadenylic acid, potassium salt), and poly(dA) (polydeoxyadenylic acid, sodium salt) were purchased from Sigma-Aldrich. (rA)₂ was purchased from Sequoia Research Products. Ammonium salts of (rA)₄ and (dA)_n, *n* = 2, 3, 4, 5, 6, 8, 12, and 18, were purchased from Midland Certified Reagent Company. All samples were used without further purification.

Generally, samples were prepared in a pH 7 phosphate buffer solution made from 25 mM Na₂HPO₄ and KH₂PO₄, and pure

water from a water ultrapurifier (NANOpure Ultrapure Water System, Barnstead International). Most experiments were performed on solutions containing NaCl at a concentration of 0.25 M. Control experiments on (dA)₂, (dA)₁₈, and polyA in phosphate buffer solutions without added salt gave identical transient absorption signals within experimental uncertainty. D₂O (deuterium oxide, 99.9 atom % D) was purchased from Sigma-Aldrich and was used unbuffered. For low pH measurements in H₂O, concentrated aqueous HCl was added dropwise to a neutral buffer solution until the desired pH was reached.

Sample concentrations were adjusted to give an absorbance of ~ 1.0 in the 1.2 mm path length cell used. All experiments were carried out at room temperature. Absorption spectra recorded before and after transient absorption measurements with a UV/vis spectrophotometer (Lambda 25, PerkinElmer) showed no evidence of sample photodegradation.

Positive-going, spike-like signals were observed from all samples around time zero. These signals arise from simultaneous absorption of one photon from both the pump and probe pulses by the water solvent and persist only as long as their temporal overlap.^{20,21} These coherent signals do not depend on the solute and were excluded from fits to the transient signals by masking data points at delay times <0.8 ps. These water-induced signals provide a useful measurement of the instrument response function (IRF),^{20,21} which was determined to be 250 fs (fwhm) for the UV-probe experiments. A Gaussian function of 250 fs fwhm was convoluted analytically with the sum of one or more exponentials and used to fit transient absorption signals using a nonlinear least-squares algorithm with global fitting capabilities. Unless otherwise specified, all uncertainties reported are twice the standard deviation (2σ , 95% confidence interval) estimated by the fitting program.

3. RESULTS

3.1. Length-Dependent Bleach Recovery Signals for DNA A Tracts. Transient absorption signals (pump 266 nm, probe 250 nm) from single-stranded adenine oligodeoxynucleotides, (dA)_{*n*}, where *n* varies between 2 and 18, are shown in Figure 1 and compared with the signal from the mononucleotide 2′-deoxyadenosine 5′-monophosphate (dAMP). The

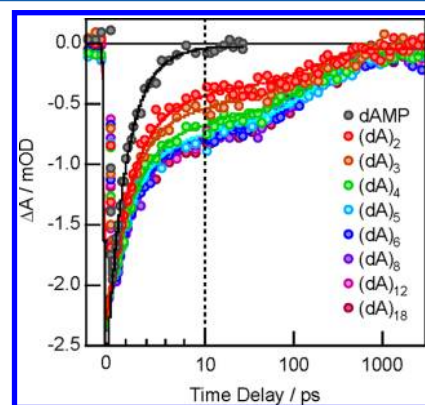


Figure 1. Back-to-back transient absorption signals of dAMP and adenine homo-oligonucleotides with 2 to 18 bases. Signals were globally fit as described in the text. In this and later figures showing transient absorption signals, the time delay axis is linear from 0 to 10 ps and logarithmic at later times. The break between linear and logarithmic scaling is shown by the dashed vertical line.

signals were recorded in back-to-back measurements on solutions having equal absorbance at the pump wavelength and with all experimental parameters, such as laser pump energy and spot size, maintained as constant as possible. These conditions ensure that the same number of initial excited states is formed in each sample. This is a requirement for the method for estimating yields that will be presented below.

The dAMP signal has decayed to zero approximately 10 ps after excitation. This decay is well described by a single exponential, and negligible improvement in the quality of fit is achieved by adding a second exponential. The oligodeoxynucleotide signals decay at short delay times on the same time scale as the dAMP signal. The fast decay is followed by a long-lived component that approaches but does not quite reach the baseline 1 ns after excitation. The long-time signals decay at the same rate for all $n \geq 2$. An excellent global fit was obtained using two exponentials plus an offset with common exponential time constants of 2.72 ± 0.06 ps and 183 ± 6 ps (solid curves in Figure 1). Fitting the dAMP bleach signal separately yields a lifetime of $\tau_1 = 2.01 \pm 0.09$ ps, which is somewhat faster than the fast component observed in the oligonucleotides. All fit parameters are summarized in Table 1.

Table 1. Best-Fit Parameters for (dA)_n Transient Absorption Signals in Figure 1^a

n	A_1	A_2	A_3
1 ^b	-2.99	=0	-0.028
2	-2.07	-0.365	-0.046
3	-1.83	-0.485	-0.045
4	-1.89	-0.570	-0.096
5	-1.76	-0.634	-0.12
6	-1.69	-0.685	-0.11
8	-1.74	-0.719	-0.092
12	-1.62	-0.698	-0.081
18	-1.47	-0.753	-0.077

^aThe (dA)_n transients were fit to the sum of two exponentials plus an offset, $A_1 \exp(-t/\tau_1) + A_2 \exp(-t/\tau_2) + A_3$, convoluted with a Gaussian of fwhm 0.25 ps to model the instrument response function. A single exponential with lifetime $\tau_1 = 2.01 \pm 0.09$ ps produced the best fit for dAMP ($n = 1$). For the (dA)_n ($n \geq 2$), the global lifetimes are $\tau_1 = 2.72 \pm 0.06$ ps and $\tau_2 = 183 \pm 6$ ps. The uncertainties in the amplitudes are approximately independent of n and equal to 0.05 (A_1), 0.02 (A_2), and 0.01 (A_3). All uncertainties are equal to the standard error (σ). ^bdAMP.

The maximum bleach amplitude near time zero is similar for all samples and does not change systematically with length. The small variation of no more than 10% that is observed is likely due to experimental difficulties in maintaining identical conditions of pump pulse energy, etc. For this reason, relative or fractional amplitudes are plotted vs n in Figure 2. The amplitude of the long-time decay component, A_2 , increases with n (circles in Figure 2), while the amplitude of the shortest lifetime component, A_1 , decreases (triangles in Figure 2).

3.2. DNA vs RNA A Tract Transients. Transient absorption signals recorded at a pump wavelength of 266 nm and a probe wavelength of 250 nm in back-to-back experiments on equal absorbance solutions of AMP, (rA)₄, and (dA)₄ are shown in Figure 3. Both the (rA)₄ and (dA)₄ signals decay biexponentially on similar time scales, but the (dA)₄ signal has greater amplitude at delay times greater than 10 ps. Best-fit parameters are listed in Table 2.

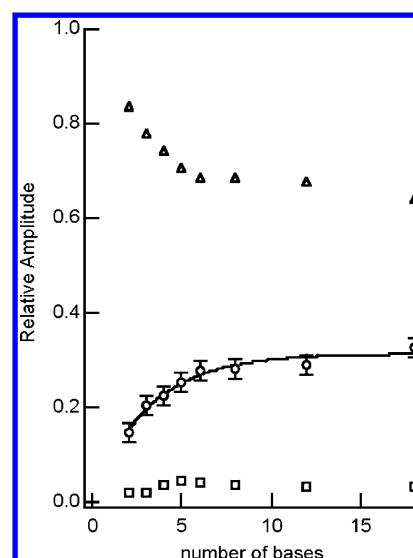


Figure 2. Relative amplitudes from global fits to (dA)_n transients in Figure 1: triangles, $A_1/\sum_i A_i$; circles, $A_2/\sum_i A_i$; squares, $A_3/\sum_i A_i$. A best-fit exponential function through the A_2 relative amplitudes is shown by the solid curve.

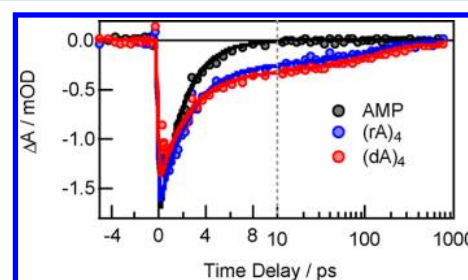


Figure 3. Back-to-back transient bleach signals for AMP, (rA)₄, and (dA)₄.

Table 2. Best-Fit Parameters for Transient Absorption Signals in Figure 3^a

sample	A_1	A_2	A_3	h_{266}^b (%)	f_g^c	f_e^c
AMP	-1.93	=0	9.0×10^{-4}			
(rA) ₄	-1.54	-0.242	-0.014	28.8	0.43	0.20
(dA) ₄	-1.17	-0.291	-0.039	32.9	0.59	0.39

^aTransients were fit to the sum of two exponentials plus an offset, $A_1 \exp(-t/\tau_1) + A_2 \exp(-t/\tau_2) + A_3$, convoluted with a Gaussian of fwhm 0.25 ps to model the instrument response function. A single exponential with lifetime $\tau_1 = 2.03 \pm 0.06$ ps produced the best fit for AMP. For (dA)₄ and (rA)₄, the global lifetimes are $\tau_1 = 2.44 \pm 0.09$ ps and $\tau_2 = 136 \pm 15$ ps. The uncertainties in the amplitudes are approximately the same for (dA)₄ and (rA)₄ and equal to 0.04 (A_1), 0.01 (A_2), and 0.01 (A_3). All uncertainties are equal to the standard error (σ). ^bPercentage hypochromicity estimated using data from ref 57, our measured absorption spectra, and a value of 15.4×10^3 M⁻¹ cm⁻¹ for the molar absorption coefficient of AMP at 260 nm. ^cDefined in eqs 1 and 2.

Normalized transient absorption signals from equal-length RNA and DNA A-tracts are compared in Figure 4. The relative amplitude of the long-time signal component is greater for each oligodeoxyribonucleotide than for the corresponding oligoribonucleotide of the same length, and this difference becomes more pronounced as n increases.

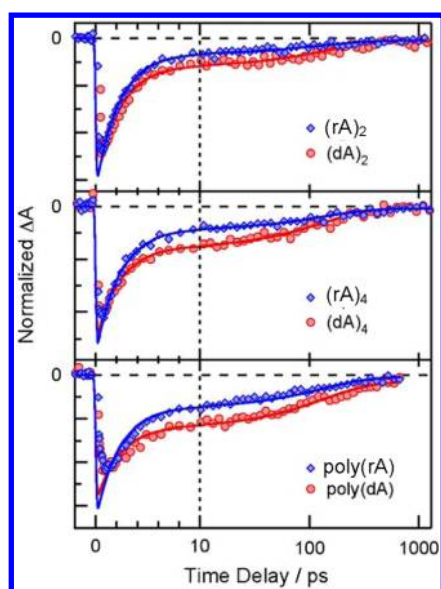


Figure 4. Comparison of normalized transient absorption signals from equal length DNA and RNA multimers: $(rA)_2$ and $(dA)_2$, top panel; $(rA)_4$ vs $(dA)_4$, middle panel; poly(rA) and poly(dA), bottom panel. The transients have been normalized to have the same amplitude near time zero.

3.3. Kinetic Isotope Effect on Bleach Recovery Signals.

Transient absorption signals (pump 266 nm, probe 250 nm) for AMP and $(rA)_4$ in H_2O and D_2O are shown in parts a and b, respectively, of Figure 5. The solid curves in Figure 5 were

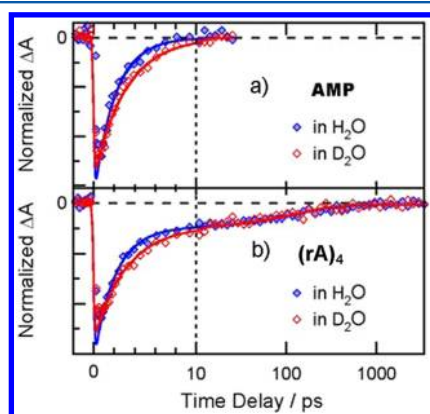


Figure 5. Transient absorption signals from (a) AMP and (b) $(rA)_4$ in H_2O and D_2O solution. The pump wavelength for these signals is 266 nm, and the probe wavelength is 250 nm. The signals have been normalized to have the same maximum bleach amplitude near time zero.

obtained by nonlinear least-squares fits to the individual transients. Parameters for the fits are listed in Table 3. In both solvents, the AMP signal decays approximately monoexponentially, while the $(rA)_4$ signal decays biexponentially. A kinetic isotope effect is seen for AMP and for the fast component in $(rA)_4$. The kinetic isotope effect ($KIE = \tau_D/\tau_H$) of 1.49 ± 0.08 measured for AMP agrees with the KIE of 1.53 ± 0.13 for $(rA)_4$ within experimental uncertainty.

3.4. pH Effect on $(dA)_2$ Lifetimes. Transient absorption signals (pump 266 nm, probe 250 nm) for $(dA)_2$ and dAMP in aqueous solution at pH 2 and pH 7 are compared in Figure 6. Biphasic bleach recovery is observed for $(dA)_2$ at pH 7 (filled

Table 3. Best-Fit Parameters for Transients in Figure 5^a

system	A_1	A_2	A_3	τ_1 (ps)	τ_2 (ps)
AMP	H_2O	-1.37		1.93 ± 0.08	
	D_2O	-1.19		2.88 ± 0.11	
A_4	H_2O	-1.02	-0.17	2.37 ± 0.14	207 ± 45
	D_2O	-0.88	-0.16	3.62 ± 0.23	170 ± 40

^aTransients were fit to the sum of two exponentials plus an offset, $A_1 \exp(-t/\tau_1) + A_2 \exp(-t/\tau_2) + A_3$, convoluted with a Gaussian of fwhm 0.25 ps to model the instrument response function. All uncertainties are equal to the standard error (σ).

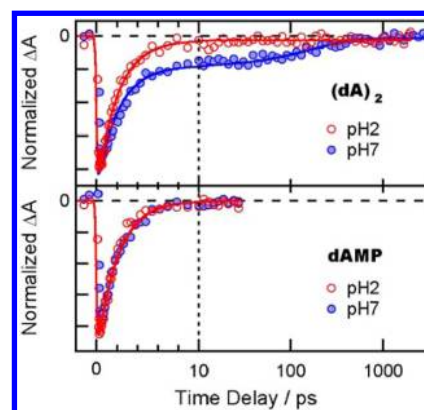


Figure 6. Transient absorption signals of $(dA)_2$ and dAMP at pH 2 and pH 7. The signals are normalized to have the same maximum bleach amplitude.

blue circles), but the long-lived decay component vanishes at pH 2 (open red circles). In contrast, the dAMP bleach recovery signals are identical within experimental uncertainty at both pH values (Figure 6, lower panel). The $(dA)_2$ signal at pH 2 decays monoexponentially with a lifetime of ~ 2 ps that agrees within experimental uncertainty with the lifetime for dAMP at pH 2 and pH 7.

4. DISCUSSION

The bleach recovery signals for $(dA)_n$ oligonucleotides recover on two widely separated time scales (see Figure 1 and Table 1). Previously, Takaya et al.⁵ observed long-lived excited states in transient absorption experiments on RNA dinucleosides. Because the same lifetime was observed in $(rA)_2$ as in much longer RNA A tracts, these authors suggested that the long-lived excited states are the same regardless of RNA A tract length and are localized on just two bases.⁵ The observation here that transient absorption signals from $(dA)_n$ oligonucleotides containing between 2 and 18 bases can be globally fit using a common set of time constants extends the earlier finding of Takaya et al.⁵ for RNA forms to A tracts with a DNA backbone. Excimers or charge-transfer states are consistent with a high degree of localization, but direct evidence for such states is still lacking, even though a number of computational studies support their existence.^{22–25}

The amplitude of the long-lived signal (A_2 in Table 1) is weakest in $(dA)_2$, is strongest in $(dA)_{18}$, and increases with the number of residues n . The graph of A_2 vs n (Figure 2) has the same shape as the graph of “exciton absorption intensity” vs n (Figure 3 in ref 17) obtained by Buchvarov et al.¹⁷ from the ratio of their transient absorption signal amplitudes recorded at

two probe wavelengths 3 ps after excitation. The solid curve through the circles in Figure 2 is a fit to a single exponential function with a decay constant of 3.2 ± 0.6 bases. This matches quantitatively the “1/e delocalization length” of 3.3 ± 0.5 bases reported in ref 17. The amplitude of the long-lived signal component from our bleach recovery transients thus varies in precisely the same way with oligomer length as the quantity obtained by Buchvarov et al.,¹⁷ from their more complex analysis of transient signals recorded at two probe wavelengths. Buchvarov et al.¹⁷ interpreted this variation as evidence of increasing excited state delocalization in longer oligomers. In the following, we show that base-stacking disorder, and not length-dependent excited state delocalization, provides the best explanation for the observed signal variation.

4.1. Evidence of Heterogeneous Kinetics in the Bleach Recovery Signals. The distinctive biexponential nature of the $(dA)_n$ bleach signals at delay times <1 ns could be due to a single kinetic scheme with transitions between two or more excited states or could result from inhomogeneous kinetics in which different oligomers in the ensemble differ in their excited-state dynamics. The latter possibility is a very reasonable starting point given the considerable structural heterogeneity expected for flexible single-stranded oligomers. Electronic excitations in DNA are built on excited states of weakly interacting nucleotides,^{26,27} so we shall look for evidence of heterogeneous excited-state dynamics at the level of individual nucleotides within oligomers.

The bleach recovery lifetimes measured here in H₂O solution for dAMP (2.01 ± 0.09 ps) and AMP (1.93 ± 0.08 ps) agree within experimental uncertainty. As reviewed elsewhere,⁴ this component, which is common to all nucleic acid monomers probed at UV wavelengths, is assigned to rate-limiting vibrational cooling following ultrafast internal conversion. The lifetime is 20% faster than the 2.4 ps vibrational cooling time reported for 9-methyladenine.²⁸ Faster cooling by the mononucleotides may be due to their greater number of hydrogen bonding sites compared to a free base such as 9-methyladenine. Vibrational-cooling rates generally increase when the number of hydrogen bonds between the solute and the solvent is increased.²⁹

Strong evidence that the long-lived signal component arises from a distinct population of excited states comes from the experiments in H₂O and D₂O. Vibrational cooling by the monomer 9-methyladenine exhibits a solvent kinetic isotope effect (KIE) with slower cooling in D₂O than in H₂O.²⁸ Here, the lifetime of the slow component for $(rA)_4$ is the same in H₂O and D₂O, but a KIE appears on the fast signal component (Figure 5 and Table 3), which agrees within experimental uncertainty with the KIE observed for AMP (Table 3). This behavior is best explained by short- and long-time signals that arise from different excited state populations. Only the rapidly decaying signal component, which is assigned to vibrational cooling following ultrafast internal conversion as in the mononucleotide solution, is influenced by the solvent's isotopic composition.

In fact, the fast signal component ($\tau_1 = 2.72 \pm 0.06$ ps) observed for the $(dA)_n$ oligomers is about 40% slower than the lifetime seen for dAMP (2.01 ± 0.09 ps). The precise reasons for this are unclear, but it could be due to a slower rate of internal conversion in the oligomer compared to the monomer. Alternatively, it is possible that the backbone as well as nearby adenine residues reduce hydration by water molecules, increasing the vibrational cooling time in the oligonucleotides

in much the same way that vibrational cooling times for a given solute increase in organic solvents compared to aqueous solution.²⁸ We conclude from the experiments in H₂O and D₂O that two distinct excited-state populations are responsible for the biphasic decays.

4.2. Quantum Yield of Long-Lived Excited States.

Earlier, we proposed a method for estimating the quantum yield of long-lived excited states of dinucleoside monophosphates from femtosecond transient absorption measurements.⁵ This model and its extension to oligomers is presented in detail in the Supporting Information. In this model, the two decay components result from two classes of nucleotides in the oligomers that give rise to either short- or long-lived excited states upon excitation. A key assumption is that those nucleotides in the oligomer that are responsible for the fast component produce the same excited-state dynamics as free nucleotides. In other words, nucleotides in $(dA)_n$ oligomers that give rise to short-lived excited states are assumed to have identical ground and excited-state absorption cross sections as the monomer dAMP. In this case, a comparison of the amplitude of the fast signal component from $(dA)_n$ with the signal amplitude of an equal absorbance solution of dAMP can be used to determine the fraction of short-lived vs long-lived excitations as shown in Supporting Information. Any energy transfer between the two kinds of excited states is ruled out.

All nucleotides in each oligomer are in their electronic ground states before interaction with the pump pulse. The fraction of nucleotides, f_g , in the oligomer solution that would yield long-lived excited states, if excited, can be estimated from eq 1, which is derived in the Supporting Information,

$$f_g = 1 - \frac{A_1}{A_1^m}(1 - h) \quad (1)$$

In eq 1, A_1 is the best-fit amplitude for the fast component from the oligomer transient absorption signal, while A_1^m is the amplitude from the single-exponential fit to the signal recorded from an AMP solution having the same absorbance at the pump wavelength, and h is the hypochromicity at the pump wavelength.

The fraction of oligomer excited states that are long-lived, f_e , is equal to

$$f_e = 1 - \frac{A_1}{A_1^m} \quad (2)$$

It was incorrectly claimed in ref 5 that the quantum yield of long-lived excited states is given by eq 1, but the correct quantum yield is actually given by eq 2, as shown in the Supporting Information. Note, however, that the authors of ref 5 correctly compared the fraction of stacked bases with values calculated from eq 1. The quantum yield of long-lived excited states, f_e , is less than f_g when h is nonzero because the nucleotides that yield long-lived excited states upon excitation have smaller absorption cross sections and are therefore excited less often than the other nucleotides. Consequently, the excited state population is enriched in excitations associated with the nucleotides responsible for short-lived excitations. Analogously, the vapor phase of a mixture of two substances differs in composition compared to the liquid phase when the substances differ in volatility.

Equations 1 and 2 were evaluated from the Table 1 fit amplitudes using the hypochromicity at the pump wavelength of 266 nm, h_{266} , estimated as described in the Supporting

Information. The results are shown in the last two columns of Table 4. The quantum yield of long-lived excited states (f_e in

Table 4. Molar Absorption Coefficient, Percentage Hypochromicity, and Yields of Long-Lived Excited States for Adenine Oligodeoxynucleotides (dA)_n^a

<i>n</i>	ϵ_λ^b (10 ³ M ⁻¹ cm ⁻¹)	λ (nm)	ϵ_{266}^c (10 ³ M ⁻¹ cm ⁻¹)	h_{266}^c (%)	f_g (%)	f_e (%)
1	15.3	259	13.33			
2	12.35	258	10.34	22.5	46	31
3	11.35	257	9.50	28.8	56	39
4	10.87	257	8.94	32.9	58	37
5	10.60	257	8.64	35.2	62	41
6	10.40	257	8.40	37.0	64	43
8	10.15	257	8.13	39.0	65	42
12	9.90 ^d	257	7.85	41.1	68	46
18	9.73 ^d	257	7.77	41.7	71	51

^a ϵ_λ is the molar absorption coefficient at wavelength λ . ϵ_{266} is the molar absorption coefficient at 266 nm. h_{266} is the hypochromicity at 266 nm. f_g is the fraction of nucleotides in the oligomer that yield long-lived excited states when excited (eq 1). f_e is the quantum yield or fraction of excited states that are long-lived (eq 2). The uncertainty in f_g and f_e is $\pm 3\%$ (2σ). ^bAt pH 8.0 from ref 40. ^cCalculated as described in the Supporting Information. ^d ϵ_λ is estimated using the linear regression method described in ref 40.

Table 4) increases with DNA A tract strand length, from 31% for (dA)₂ to 51% for (dA)₁₈. In other words, about 1 in 3 excitations produces a long-lived excited state for (dA)₂, while approximately every other excitation in (dA)₁₈ is long-lived.

4.3. Base Stacking Is Responsible for Heterogeneous Kinetics. We propose that base stacking is the physical effect responsible for the kinetic heterogeneity seen in the (dA)_n oligomers. Stacked bases are responsible for the long-lived excited states, while unstacked bases give rise to the monomer-like vibrational cooling signal seen at delay times <10 ps. The pH-dependent (dA)₂ transients provide new evidence that base stacking is required for the formation of long-lived excited states.^{5,6} For (dA)₂, $pK_{a,1}$ is 3.89 and $pK_{a,2}$ is 3.02.³⁰ At pH 2, (dA)₂ is doubly protonated and unstacked by Coulombic repulsion.^{31–34} Figure 6 shows that this fully unstacked structure lacks any long-lived signal.

The pK_a of dAMP is 3.97 ± 0.02 ,³⁵ and this corresponds to protonation of adenine at N1. The ground-state recovery signal of dAMP is identical at pH 2 and 7 (Figure 6, lower panel), indicating that protonation does not alter the rate of nonradiative decay by the monomer. This agrees with earlier work showing that transient absorption signals (pump 260 nm, probe 570 nm) are very similar for AMP at pH 3.7, 5.4, and 7.0.⁶ The elimination of the long-lived signal at low pH is therefore due to a change in conformation and not due to a change in the electronic structure of the adenine chromophore. Significantly, long-lived excited states are still observed at low pH in poly(rA)⁶ and poly(dC).³⁶ Both systems adopt non-Watson–Crick double-stranded forms, suggesting that it is not protonation of the chromophores *per se* that quenches long-lived excited states but rather the loss of base stacking.

A wide variety of experimental techniques provide clear evidence that bases in single-stranded DNA and RNA sequences can stack with nearest neighbors, forming helical segments in which the conformation resembles that of a single strand in a duplex nucleic acid. Single-stranded oligomers and polymers containing runs of adenine bases exhibit a higher

degree of stacking than other sequences. Thus, sedimentation velocity analysis indicates that dA homo-oligonucleotides have more extended shapes than dT and dC homosequences because of the strong tendency of dA sequences to form partially ordered helices.³⁷ Base stacking also affects the elasticity of single-stranded DNA and stretching experiments provide evidence of substantial base-stacked structure.^{38,39} UV hypochromicity⁴⁰ and circular dichroism experiments⁴¹ conducted as a function of temperature provide further evidence of base stacking in polyadenylates.

Base stacking in a single strand involves interactions primarily between nearest-neighbor bases and exhibits little cooperativity in contrast to α helix formation by polypeptides.⁴² Consequently, the structure of an oligonucleotide such as (dA)_n in solution is thought to be that of a rod–coil multiblock copolymer possessing short, rodlike helical domains at room temperature.^{39,43} Base stacks in adenine homo-oligonucleotides in room-temperature solution thus constitute a distribution of helical domains. Evidence further indicates that the average domain length is generally considerably shorter in length than the oligomer itself.⁴³

In the early 1960s, Applequist and Damle showed that a one-dimensional Ising model can successfully model length-dependent hypochromicity in RNA A tracts.⁴³ In this model, stacking is assumed to involve pairwise interactions between a base and one or both of its two nearest neighbors. A stacking relationship between any pair of adjacent bases is referred to as an “S bond”,⁴³ and stacking in an oligomer of *n* bases is therefore specified by a binary number of length *n* – 1, with 1s and 0s denoting the presence and absence of S bonds, respectively.

Applequist and Damle derived exact solutions for the distribution of helical stacks.⁴³ They included in their model a cooperativity parameter, σ , which makes it more favorable to add a new S bond to an existing base stack. However, their results,⁴³ and those of others,^{41,44–47} indicate that stacking in single-stranded nucleic acids is largely noncooperative. We therefore restrict our discussion of the Applequist and Damle theory to the fully noncooperative case in which the σ parameter from ref 43 is set to unity. In this case, base stacking is fully described by the equilibrium constant *s* describing the two-state equilibrium for forming an S bond. The resulting expressions are mathematically simpler and make it easier to pinpoint the effect of oligomer length on base stacking, an effect that is little changed by the addition of a modest degree of cooperativity to the model.

The fraction of S bonds, *f*, is independent of the number of bases *N* in an oligomer and is given by

$$f = \frac{s}{s + 1} \quad (3)$$

At the transition midpoint, *s* = 1 and *f* = 0.5, indicating the formation of half of all possible S bonds in the ensemble of oligomers. Base stacking is effectively treated as a two-state equilibrium. Although this can be criticized, a two-state model successfully accounts for data from a variety of experiments that are sensitive to base stacking.⁴⁸

The distribution of base stacks by length varies with temperature due to the temperature dependence of the equilibrium constant *s*. The average length of a base stack, \bar{L} , is given at any particular temperature in the noncooperative limit by

$$\bar{L} = \frac{n-1}{n-1-f(n-2)} = \frac{(n-1)(1+s)}{n-1+s} \quad (4)$$

Even though the same thermodynamic parameters govern the melting of the dimer and longer oligomers,⁴¹ the fraction of bases present in stacks is nonetheless dependent on oligomer length. The fraction of bases present in stacks of two or more bases, f_b , varies with n , the number of bases, according to

$$f_b(n) = f(2-f) + \frac{2f(f-1)}{n} \quad (5)$$

The fraction of stacked bases depends on oligomer length as long as f is less than unity because terminal bases, which have only a single nearest neighbor, are less likely to be found in a stack than interior residues, which can stack with either of two neighboring bases. For the same reason, the first and last coin tossed in a sequence of n tosses have a reduced probability of occurring in a run of two or more heads.

In order to test whether base stacking is the physical effect that causes an excited state in an oligomer to be long-lived, we fit the measured f_g values (Table 3) to the right-hand side of eq 5 (Figure 7). The excellent quality of the fit, which depends on

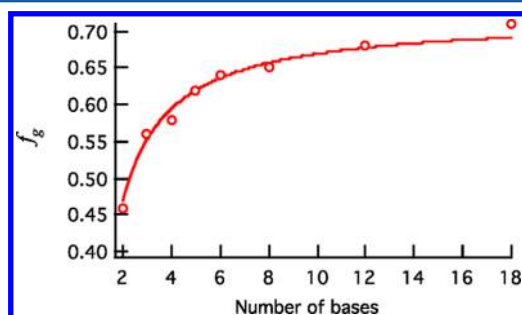


Figure 7. f_g from Table 3 vs $(dA)_n$ oligonucleotide length (red circles). The smooth curve is a fit to eq 5.

the single parameter, f , shows that the probability of forming a long-lived state varies in the same manner with oligomer length as the probability that any base in the oligomer is present in a base stack. This is a strong indication that base stacking determines whether excitations in single-stranded DNA are long-lived or not.

The best-fit value of f is 0.470 ± 0.009 (95% confidence), suggesting that the probability of stacking in the dimer $(dA)_2$ is approximately 0.5 under our experimental conditions. Using this value of f in eq 4 predicts that the average length of a stacked domain in $(dA)_{18}$ is just 1.8 bases long even though 69% of all bases are present in stacks according to eq 5. These numbers reinforce the conclusion that even when most bases are stacked there can still be a significant degree of base stacking disorder.

Thermodynamic parameters determined in temperature-dependent circular dichroism experiments by Olsthoorn et al.⁴⁹ and by Kang et al.⁵⁰ predict a stacking fraction for $(dA)_2$ of 72% and 64%, respectively, at 25 °C. The value of 46% (Table 4) obtained from this analysis is lower than either of these estimates. Given the reasonable possibility of a continuum of stacked and unstacked states, it is possible that different techniques are sensitive to base stacking in different ways. Although our low pH results on $(dA)_2$ strongly argue that long-lived excited states cannot be formed in the absence of base stacking, it is possible that some excitations in stacks could

decay via ultrafast internal conversion.¹¹ The possibility of two relaxation channels in base stacks, one ultrafast and one taking place on longer time scales, would cause the yield of long-lived excited states to be lower than expected.

Base stacking also explains why RNA A tracts like $(rA)_4$ have lower amplitude for the long-lived signal component than equal length DNA A tracts (Figures 3 and 4). Table 2 shows that both f_g and f_e are greater in $(dA)_4$ than in $(rA)_4$. Hypochromicity and NMR results indicate that the RNA dimer $(rA)_2$ is more stacked than the DNA dimer $(dA)_2$.⁵¹ It has been shown in ribonucleoside monophosphates that interaction of the 2' hydroxyl group of 5' ribose with adjacent base and sugar moieties destabilizes stacking.⁵² Because stacking is noncooperative, the reduced propensity for stacking in the dimer carries over to the longer oligomers.

4.4. Transient Absorption Signals and Exciton Delocalization. As pointed out earlier, the signal shown in Figure 3 of ref 17 varies with the number of residues in the same way as the transient absorption signal amplitudes shown by the circles in Figure 2 of this article. Buchvarov et al.¹⁷ assigned their signals to exciton absorption intensity, which increases at first with n for shorter sequences but then saturates, becoming constant for sequences with 10 or more bases. The authors fit an exponential to the data in their graph to obtain a "1/e delocalization length" of 3.3 ± 0.5 bases. Other researchers have interpreted this result in contradictory ways. Onidas et al.⁵³ wrote that "the degree of delocalization may reach 10 base pairs". Tonzani and Schatz⁵⁴ equated the "1/e delocalization length" of 3.3 with the limiting or saturation value of the delocalization seen for long sequences. Citing ref 17, Improta wrote that theory and experiment agree that absorption produces excited states that are delocalized over 4 to 6 stacked bases.⁵⁵

In our view, uncertainty about the meaning of "1/e delocalization length" is responsible for this confusion. This nomenclature and the discussion in the Buchvarov et al. paper suggests that these authors fit their transient absorption signal amplitudes to an expression of the form

$$f_n = b - ae^{-n/d} \quad (6)$$

where f_n is the oscillator strength for an exciton in an oligomer of n residues, d is the 1/e delocalization length, and a and b are fitting parameters. This functional form shows that the 1/e delocalization length, d , emphasized by Buchvarov et al.,¹⁷ does not measure the absolute exciton delocalization length but merely its rate of change.

Regardless of the confusion over the meaning of the 1/e delocalization length of 3.3 bases reported in ref 17, the critical issue is whether the approach described by Buchvarov et al.¹⁷ can measure the delocalization length of DNA excitons. Buchvarov et al.¹⁷ attributed the signal variation seen in their experiments to excited-state delocalization. They assumed that the increasing signal amplitudes observed for longer oligomers are a manifestation of the larger absorption cross sections expected for excitons that are delocalized over a larger number of bases. However, transient absorption signals depend on both populations and absorption cross sections. The assumption by Buchvarov et al.¹⁷ that "the effective number of stacked adenine dimers is approximately constant" in all oligomers regardless of length n is contradicted by the structural models discussed earlier. We propose that absorption cross sections are the same for the long-lived excited states regardless of the number of

residues and it is the populations that vary with oligomer length. Our results show that the transient absorption signal amplitudes vary in the same way with n as the fraction of stacked bases. This is strong evidence that the variation in transient absorption signal amplitudes results from excited state populations that are modulated by base stacking disorder.

The existence of excitons resulting from electronic coupling of proximal nucleobases in DNA is strongly supported by computational studies,^{27,54,56} and we wish to stress that our study does not refute the existence of such states. The computational studies suggest that excitons are delocalized over several bases or, in other words, over distances that are rather similar to the average domain length in room-temperature A tracts. This raises the question of whether structural disorder is the limiting factor in the delocalization of electronic energy. This is likely to be true, but we suspect that past transient absorption studies, including ours, lack sufficient time resolution to detect what is likely to be an extremely rapid transition (<100 fs) from initial excitonic states to the long-lived excited states. Buchvarov et al.¹⁷ analyzed their transient absorption signals 3 ps after the pump pulse, but the fact that (dA)₂ and the much longer poly(dA) have identical long-time signals strongly suggests that excited states are already localized by 3 ps. We conclude that transient absorption signal amplitudes measured several picoseconds after excitation are insensitive to exciton delocalization in DNA. Probing the transition from initial delocalized excitons to the slowly relaxing excited states seen in these experiments will require a careful examination of signals acquired with still higher time resolution.

5. CONCLUSIONS

Femtosecond transient absorption experiments on DNA and RNA A tracts containing a variable number of residues have provided new insights about excited-state dynamics in base multimers. The biexponentially decaying transient absorption bleach signals measured for homo-oligomers of adenine are shown to be the result of heterogeneous kinetics. The short-lived signal component exhibits a similar solvent kinetic isotope effect as monomeric adenine and is assigned to vibrational cooling by unstacked nucleotides. The long-lived signal component arises from excitations localized in stacked bases. This is clearly established by the complete elimination of the long-lived signal in the fully unstacked conformation of (rA)₂, which is present at low pH.

The amplitude of the long-lived signal component seen in transient absorption bleach signals increases systematically with the number of residues in homo-oligomers of adenine. We have presented a simple model for calculating the fraction of nucleotides that yield long-lived excited states upon absorption. This fraction increases with the number of residues in the same way that the fraction of stacked bases is predicted to increase according to a model of noncooperative stacking. Furthermore, the number of nucleotides that yield long-lived excited states is greater in DNA than in RNA oligomers of the same length. Both observations underscore the critical role played by base stacking in causing slow nonradiative decay in single-stranded nucleic acids.

A central theme that emerges from this study is the profound sensitivity of excited-state dynamics in nucleobase multimers to structure. A major conclusion is that even "simple" systems such as these single stranded homo-oligonucleotides exhibit substantial structural heterogeneity that must be accounted for by any electronic structure model. Base-stacking disorder fully

accounts for the observed signal variation without any need to invoke delocalized excitons. Indeed, the evidence presented here suggests that, even down to the earliest times probed in these experiments (~1 ps), initial excitons formed by the pump pulse, whatever their precise character, have decayed away to localized excitations.

■ ASSOCIATED CONTENT

Supporting Information

A detailed model for estimating the quantum yields of long-lived excited states in single-stranded homo-oligonucleotides and a description of percentage hypochromicity values for (dA)_n oligomers. This material is available free of charge via the Internet at <http://pubs.acs.org>.

■ AUTHOR INFORMATION

Corresponding Author

*E-mail: bkohler@montana.edu. Telephone: (406) 994-7931. Fax: (406) 994-5407.

Present Address

[§]Department of Chemistry, University of Wisconsin—Madison, 1101 University Avenue, Madison, WI 53703, and PhaseTech Spectroscopy, Inc., 2810 Crossroads Dr., Suite 4000, Madison, WI 53718.

Notes

The authors declare no competing financial interest.

■ ACKNOWLEDGMENTS

This work was made possible by grants from the National Science Foundation (CHE-0809754, CHE-1005447). Measurements were performed in Ohio State's Center for Chemical and Biophysical Dynamics, using equipment funded by the National Science Foundation and the Ohio Board of Regents.

■ REFERENCES

- (1) Crespo-Hernández, C. E.; Cohen, B.; Hare, P. M.; Kohler, B. *Chem. Rev.* **2004**, *104*, 1977–2019.
- (2) Markovitsi, D.; Gustavsson, T.; Talbot, F. *Photochem., Photobiol. Sci.* **2007**, *6*, 717–724.
- (3) Middleton, C. T.; de La Harpe, K.; Su, C.; Law, Y. K.; Crespo-Hernández, C. E.; Kohler, B. *Annu. Rev. Phys. Chem.* **2009**, *60*, 217–239.
- (4) Kohler, B. *J. Phys. Chem. Lett.* **2010**, *1*, 2047–2053.
- (5) Takaya, T.; Su, C.; de La Harpe, K.; Crespo-Hernández, C. E.; Kohler, B. *Proc. Natl. Acad. Sci. U.S.A.* **2008**, *105*, 10285–10290.
- (6) Crespo-Hernández, C. E.; Kohler, B. *J. Phys. Chem. B* **2004**, *108*, 11182–11188.
- (7) Crespo-Hernández, C. E.; Cohen, B.; Kohler, B. *Nature* **2005**, *436*, 1141–1144.
- (8) Crespo-Hernández, C. E.; de La Harpe, K.; Kohler, B. *J. Am. Chem. Soc.* **2008**, *130*, 10844–10845.
- (9) Schwalb, N. K.; Temps, F. *Science* **2008**, *322*, 243–245.
- (10) Kwok, W. M.; Ma, C. S.; Phillips, D. L. *J. Phys. Chem. B* **2009**, *113*, 11527–11534.
- (11) de La Harpe, K.; Kohler, B. *J. Phys. Chem. Lett.* **2011**, *2*, 133–138.
- (12) Smith, V. R.; Samoylova, E.; Ritze, H. H.; Radloff, W.; Schultz, T. *Phys. Chem. Chem. Phys.* **2010**, *12*, 9632–9636.
- (13) Vayá, I.; Miannay, F.-A.; Gustavsson, T.; Markovitsi, D. *ChemPhysChem* **2010**, *11*, 987–989.
- (14) Vayá, I.; Gustavsson, T.; Miannay, F. A.; Douki, T.; Markovitsi, D. *J. Am. Chem. Soc.* **2010**, *132*, 11834–11835.
- (15) Vayá, I.; Chaugenet-Barret, P.; Gustavsson, T.; Zikich, D.; Kotlyar, A. B.; Markovitsi, D. *Photochem., Photobiol. Sci.* **2010**, *9*, 1193–1195.

- (16) Kwok, W.-M.; Ma, C.; Phillips, D. L. *J. Am. Chem. Soc.* **2006**, *128*, 11894–11905.
- (17) Buchvarov, I.; Wang, Q.; Raytchev, M.; Trifonov, A.; Fiebig, T. *Proc. Natl. Acad. Sci. U.S.A.* **2007**, *104*, 4794–4797.
- (18) Conti, I.; Altoè, P.; Stenta, M.; Garavelli, M.; Orlandi, G. *Phys. Chem. Chem. Phys.* **2010**, *12*, 5016–5023.
- (19) IUPAC-IUB Commission on Biological Nomenclature. *Pure Appl. Chem.* **1974**, *40*, 277–290.
- (20) Reuther, A.; Laubereau, A.; Nikogosyan, D. N. *Opt. Commun.* **1997**, *141*, 180–184.
- (21) Rasmusson, M.; Tarnovsky, A. N.; Åkesson, E.; Sundström, V. *Chem. Phys. Lett.* **2001**, *335*, 201–208.
- (22) Lange, A. W.; Herbert, J. M. *J. Am. Chem. Soc.* **2009**, *131*, 3913–3922.
- (23) Santoro, F.; Barone, V.; Improta, R. *J. Am. Chem. Soc.* **2009**, *131*, 15232–15245.
- (24) Santoro, F.; Barone, V.; Lami, A.; Improta, R. *Phys. Chem. Chem. Phys.* **2010**, *12*, 4934–4948.
- (25) Aquino, A. J. A.; Nachtigallova, D.; Hobza, P.; Truhlar, D. G.; Hattig, C.; Lischka, H. *J. Comput. Chem.* **2011**, *32*, 1217–1227.
- (26) Tinoco, I., Jr. *J. Am. Chem. Soc.* **1960**, *82*, 4785–4790.
- (27) Bouvier, B.; Gustavsson, T.; Markovitsi, D.; Millié, P. *Chem. Phys.* **2002**, *275*, 75–92.
- (28) Middleton, C. T.; Cohen, B.; Kohler, B. *J. Phys. Chem. A* **2007**, *111*, 10460–10467.
- (29) Kovalenko, S. A.; Schanz, R.; Hennig, H.; Ernsting, N. P. *J. Chem. Phys.* **2001**, *115*, 3256–3273.
- (30) Ogasawara, N.; Inoue, Y. *J. Am. Chem. Soc.* **1976**, *98*, 7048–7053.
- (31) Warshaw, M. M.; Tinoco, I., Jr. *J. Mol. Biol.* **1965**, *13*, 54–64.
- (32) Simpkins, H.; Richards, E. G. *Biochemistry* **1967**, *6*, 2513–2520.
- (33) Johnson, N. P.; Schleich, T. *Biochemistry* **1974**, *13*, 981–987.
- (34) Ogasawara, N.; Inoue, Y. *J. Am. Chem. Soc.* **1976**, *98*, 7054–7060.
- (35) Mucha, A.; Knobloch, B.; Jezowska-Bojczuk, M.; Kozłowski, H.; Sigel, R. K. O. *Chem.—Eur. J.* **2008**, *14*, 6663–6671.
- (36) Cohen, B.; Larson, M. H.; Kohler, B. *Chem. Phys.* **2008**, *350*, 165–174.
- (37) Hatters, D. M.; Wilson, L.; Atcliffe, B. W.; Mulhern, T. D.; Guzzo-Pernell, N.; Howlett, G. J. *Biophys. J.* **2001**, *81*, 371–381.
- (38) Ke, C.; Humeniuk, M.; S-Gracz, H.; Marszalek, P. E. *Phys. Rev. Lett.* **2007**, *99*, 018302–018304.
- (39) Seol, Y.; Skinner, G. M.; Visscher, K.; Buhot, A.; Halperin, A. *Phys. Rev. Lett.* **2007**, *98*, 158103–158104.
- (40) Cassani, G. R.; Bollum, F. J. *Biochemistry* **1969**, *8*, 3928–3936.
- (41) Brahms, J.; Michelson, A. M.; van Holde, K. E. *J. Mol. Biol.* **1966**, *15*, 467–488.
- (42) Buhot, A.; Halperin, A. *Phys. Rev. E* **2004**, *70*, No. 020902-1-4.
- (43) Applequist, J.; Damle, V. J. *J. Am. Chem. Soc.* **1966**, *88*, 3895–3900.
- (44) Leng, M.; Felsenfeld, G. *J. Mol. Biol.* **1966**, *15*, 455–466.
- (45) Epand, R. M.; Scheraga, H. A. *J. Am. Chem. Soc.* **1967**, *89*, 3888–3892.
- (46) Scovell, W. M. *Biopolymers* **1978**, *17*, 969–984.
- (47) Holbrook, J. A.; Capp, M. W.; Saecker, R. M.; Record, M. T. *Biochemistry* **1999**, *38*, 8409–8422.
- (48) Powell, J. T.; Richards, E. G.; Gratzer, W. B. *Biopolymers* **1972**, *11*, 235–250.
- (49) Olsthoorn, C. S. M.; Bostelaar, L. J.; De Rooij, J. F. M.; Van Boom, J. H.; Altona, C. *Eur. J. Biochem.* **1981**, *115*, 309–321.
- (50) Kang, H.; Chou, P. J.; Johnson, W. C., Jr.; Weller, D.; Huang, S. B.; Summerton, J. E. *Biopolymers* **1992**, *32*, 1351–1363.
- (51) Kondo, N. S.; Fang, K. N.; Miller, P. S.; Ts'o, P. O. P. *Biochemistry* **1972**, *11*, 1991–2003.
- (52) Norberg, J.; Nilsson, L. *J. Am. Chem. Soc.* **1995**, *117*, 10832–10840.
- (53) Onidas, D.; Gustavsson, T.; Lazzarotto, E.; Markovitsi, D. *J. Phys. Chem. B* **2007**, *111*, 9644–9650.
- (54) Tonzani, S.; Schatz, G. C. *J. Am. Chem. Soc.* **2008**, *130*, 7607–7612.
- (55) Improta, R.; Santoro, F.; Barone, V.; Lami, A. *J. Phys. Chem. A* **2009**, *113*, 15346–15354.
- (56) Emanuele, E.; Markovitsi, D.; Millie, P.; Zakrzewska, K. *ChemPhysChem* **2005**, *6*, 1387–1393.
- (57) Pratt, A. W.; Toal, J. N.; Rushizky, G. W.; Sober, H. A. *Biochemistry* **1964**, *3*, 1831–1837.